



HAL
open science

Advancing SiC Coatings of Short-Fiber Using Triethylsilane: Insights from FB-CVD Deposition Process

Thomas Da Calva Mouillevois

► **To cite this version:**

Thomas Da Calva Mouillevois. Advancing SiC Coatings of Short-Fiber Using Triethylsilane: Insights from FB-CVD Deposition Process. Advanced Materials Technologies, 2025, 10.1002/admt.202401678 . hal-04912221

HAL Id: hal-04912221

<https://hal.science/hal-04912221v1>

Submitted on 26 Jan 2025

HAL is a multi-disciplinary open access archive for the deposit and dissemination of scientific research documents, whether they are published or not. The documents may come from teaching and research institutions in France or abroad, or from public or private research centers.

L'archive ouverte pluridisciplinaire **HAL**, est destinée au dépôt et à la diffusion de documents scientifiques de niveau recherche, publiés ou non, émanant des établissements d'enseignement et de recherche français ou étrangers, des laboratoires publics ou privés.

Advancing SiC Coatings of Short-Fiber Using Triethylsilane: Insights from FB-CVD Deposition Process

CRediT authorship contribution statement

- 1st author: **Thomas DA CALVA MOUILLEVOIS**^{1,2} (corresponding author): dacalva@lcts.u-bordeaux.fr, Conceptualization, Methodology, Formal analysis, Investigation, Validation, Writing - Original Draft, Writing - Review & Editing, Visualization.

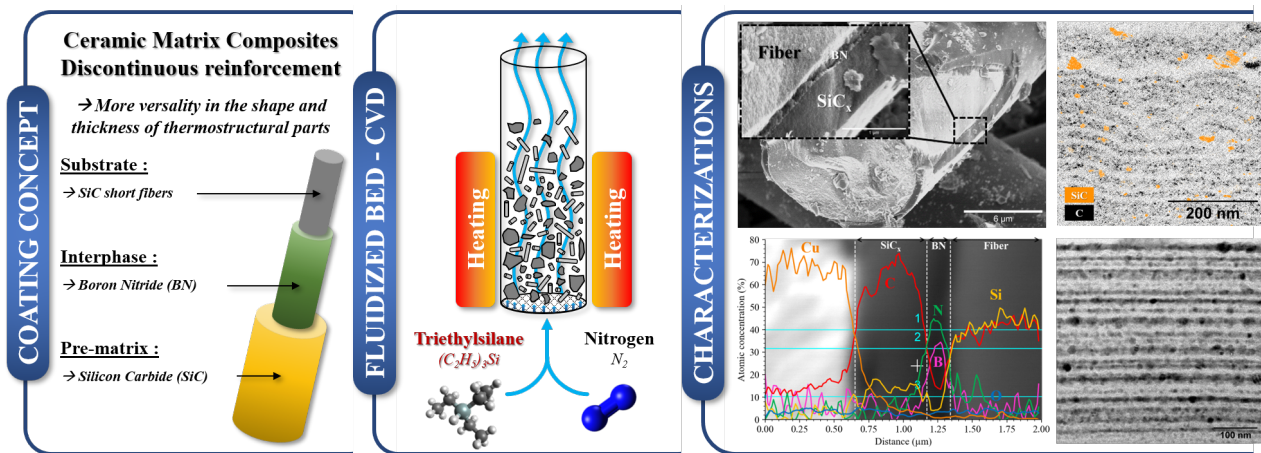
¹ ThermoStructural Composites Laboratory, CNRS – SAFRAN – CEA – University of Bordeaux, 3 Allée de la Boétie, 33600 Pessac, France

² University of Bordeaux, 351 Cour de la Libération, 33400 Talence, France

Highlights

- Uniform and robust SiC coating on short fibers by FB-CVD.
- Use of triethylsilane as a safer precursor compared to halogenated alternatives.
- Demonstration of a multi-layer interphase/pre-matrix deposit on powdered substrate.
- Stratified structure of the SiC coating with alternating carbon-rich and silicon-rich zones.
- Potential of the FB-CVD technology in particle reinforcement coatings for composites.

Graphical Abstract



Abstract

This article investigates the application of triethylsilane (TES) as a non-halogenated and less hazardous precursor in the Fluidized Bed – Chemical Vapor Deposition (FB-CVD) process for depositing silicon carbide (SiC) on short fibers. The study focuses on characterizing the pre-matrix SiC coating on an interphase boron nitride (BN) layer, aiming to enhance the understanding of these coatings for potential use in short-fiber-reinforced silicon carbide ceramic matrix composites (SiC/SiC CMCs). The FB-CVD process is explored as a promising method for coating short fibers, offering an innovative approach to enhance the applicability of discontinuous reinforced SiC/SiC CMCs. The study employs various characterization techniques, including Scanning Electron Microscopy (SEM), Energy Dispersive Spectroscopy (EDX), Auger Electron Spectroscopy (AES), X-ray Photoelectron Spectroscopy (XPS) and Transmission Electron Microscopy (TEM), to analyze the coated fibers comprehensively. Results indicate the uniformity and robustness of the SiC coating, with particular attention to preserving the underlying BN layer. The study reveals a distinctive stratified structure in the SiC deposit, alternating between carbon-rich and silicon-rich zones. The analysis of the SiC_x atomic composition through Auger spectroscopy and the atomic environment through XPS provides valuable insights. The research demonstrates the potential of TES as a precursor for SiC coating. These findings contribute to advancing the understanding of FB-CVD processes for short-fiber coating, offering a pathway to tailor coatings for improved effectiveness in short-fiber-reinforced SiC/SiC composites. The study opens avenues for further optimization strategies to achieve precise control over coating properties.

Keywords

Fluidized Bed, Chemical Vapor Deposition, Thin Film, Physico-chemical Characterization, Silicon Carbide

Colors for figures

For a proper readability of the figures, all require color printing.

1. Introduction

35 The aerospace industry is increasingly using silicon carbide fiber-reinforced ceramic matrix composites (SiC/SiC CMCs) to fulfill their requirements for
lightweight materials, superior mechanical strength, and thermal stability [1–3]. Among these materials, short fiber-reinforced CMCs have gained
considerable attention for their properties, which enable an optimal balance of weight, mechanical strength, and resistance to harsh environmental
40 conditions [4,5]. Moreover, such materials have the potential to be applied to thermostructural parts with complex shapes or low thicknesses. To achieve
optimal performance, short fibers must undergo coating with an interphase and pre-matrix layers. The interphase layer is crucial for the composite to
reach a pseudo-ductile behavior and the pre-matrix layer is needed to protect the fibers exposed to liquid silicon when densified by melt infiltration (MI).
While interphase coatings are made of pyrolytic carbon [6] or, more recently, turbostratic boron nitride [7] and act as a mechanical fuse, pre-matrix
coatings can be made of silicon carbide to be chemically compatible with the matrix densification process. As a result, these components have significant
potential to improve the performance and durability of materials exposed to severe conditions [8]. While the specifications for long fibers, which are
typically woven, coating are well understood and managed [9–14], there is a need to re-evaluate the surface engineering to accommodate short fibers.
45 This tailoring is essential to improve the overall effectiveness of short-fibers SiC/SiC composites.

One promising method for coating short fibers is the Fluidized Bed – Chemical Vapor Deposition (FB-CVD) process [15,16]. This technique offers an
innovative approach for short fiber coating. FB-CVD has a notable advantage in depositing ceramics layers on particulate substrates [17–19], especially
short fibers [16]. To ensure resistance against the matrix densifications made by the Melt Infiltration (MI) process, it is necessary to have a uniform
coating all over the surface of the particles. Therefore, critical considerations during synthesis is to uniformly coat the substrates, control the adhesion of
50 the coating, as well as the interlayer adhesion in multilayer coatings. Halogenated precursors such as trichloride boron (BCl_3) [20] or trifluoride boron
(BF_3) [21] mixed with ammonia (NH_3) are commonly used in the industry for BN interphase coatings, while methyltrichlorosilane (SiCl_3CH_3) [22] or
silane/hydrocarbons mixture [23] are used for SiC pre-matrix coatings. Although these precursors exhibit conformal deposition, they also generate
undesirable byproducts which cause equipment degradation and require expensive cold or cryogenic traps or are highly hazardous and present a potential
danger to the experimenter or the environment due to their toxicity. To reduce these disadvantages, non-halogenated and less hazardous precursors are
55 under investigation. This study focuses on the use of triethylsilane ($(\text{C}_2\text{H}_5)_3\text{Si}$, TES) as a single-source SiC precursor. Triethylsilane is liquid at room
temperature and offer potential advantages in pre-matrix coatings. Triethylsilane precursor has been used with plasma-enhanced CVD process to prepare
silicon-containing films for transistor devices [24], amorphous silicon carbonitride ($\text{a-Si}_{1-x}\text{C}_x\text{:H}$) films [25], silicon nitride films [26], amorphous
hydrogenated silicon carbonitride (a-SiCN:H) films [27,28], or with repeated cycle of CVD and oxidation processes to prepare SiO_2 films [29]. All of the
studies suggest that the coatings were amorphous, and in most SiC deposits, carbon exceeds silicon.

60 This article investigates the potential use of TES for the FB-CVD deposition of silicon carbide on short fibers, with particular emphasis on the
characterization of the pre-matrix SiC coating on an interphase BN layer. Understanding these coatings is crucial for assessing their effectiveness as
reinforcing constituents in SiC/SiC composites, resulting in significant advancements in high-performance materials technology.

2. Experimental procedure and characterizations

2.1. FB-CVD coating

65 The coatings are applied through a fluidized bed reactor, further description of the reactor can be found in [15]. To protect the reactor's sensitive
components, the column is initially filled with 580 g of zirconia beads with a diameter of 0.5 mm [30], raising the charge to the heating elements' height.
Next, a mixture of SIKA® TECH silicon carbide (SiC) powders from Fiven and desized SiC Hi-Nicalon type S short fibers from NGS Advanced Fibers
Co., Ltd is added into the fluidization column. The mixture is mixed and maintained in the fluidized bed for several minutes at a high nitrogen flow rate
exceeding 2000 sccm. The column is then placed under vacuum for several hours before being raised to 200 mbar for the CVD process. The liquid
70 precursor (TES) is then fed under pressure into a commercial evaporator from 2M Process. The evaporator combines the liquid precursor with nitrogen
in aerosol form. The aerosol is heated inside the evaporator cell and transported to the plant via an insulated line using the gas stream. The heating
elements are gradually warmed to the coating temperature (850°C) and then stabilized before the injection of the precursor. At the outlet, precursor
decomposition by-products are trapped by a series of cold traps and particle filters to prevent fine particles from entering the pumping system. Following
the coating process, the charge is recovered, sieved, and analyzed. The SiC coating is applied to a BN ex-TEAB interphase previously described in [31].
75 This initial coating maintained stoichiometry with a low carbon content, despite utilizing a precursor rich in carbon. The thickness of the coating measured

approximately 100 nm. In the following, silicon carbide deposition will be referred to as "SiC_x" due to its non-stoichiometric silicon and carbon content ($x > 1$).

2.2. High temperature treatments

Following the CVD coating process, the coated particles were subjected to heat treatment in a horizontal tube furnace. The furnace was heated to a temperature of 1450°C for a duration of 2 hours under an argon atmosphere and at atmospheric pressure, monitored via pyrometric sighting. The coated particles were contained within a graphite crucible and covered by a pierced graphite disk to allow for release of any pyrolysis gases. The crucibles are initially cleansed and subjected to vacuum heat treatment in order to avoid any contamination.

2.3. Characterizations techniques

2.3.1. SEM/EDX analysis

The coatings were analyzed via Scanning Electron Microscopy (SEM), using the FEI Quanta 400 FEG V3® and the Hitachi S4500 FEG SEM instruments. Microscopic images were captured under specific acceleration voltages, with the FEI Quanta operating at 5 kV and the Hitachi at 3 kV, to maximize resolution and reduce potential interference. The X-ray analysis was conducted utilizing the FEI Quanta SEM, which is equipped with a 100 mm² EDX Ultim Premium detector, and operated at a minimal acceleration voltage of 5 keV. This method was selected to enable extensive surface analysis, specifically appropriate for thin coatings. Before the EDX-SEM analysis, the particles underwent a preparation process consisting of mixing coated particles with copper powder, palletization, sectioning and polishing. This method yielded cross-sectional views of the coatings with better resolution.

2.3.2. Auger analysis

The study employed Auger Electron Spectroscopy (AES) using an ULVAC-Phi AUGER PHI 710 nanosonde equipped with an Ar⁺ ion gun. The nanosonde had a diameter of 10 nm and an interaction depth of 5 nm. To alleviate charge-induced artifacts, a sample inclination was applied. AES was achieved through incident electrons (5-25 keV) similar to Scanning Electron Microscopy. Emitted electron spectra ranging from 50 eV to 2.5 keV were recorded to identify elements and analyze concentrations with a precision of 5%_{at}. The ULVAC-Phi AUGER PHI 710 nanosonde, coupled with an Ar⁺ ion gun for creating depth profiles, was used to obtain high-resolution spectra.

2.3.3. XPS analysis

In order to conduct X-ray Photoelectron Spectroscopy (XPS) surface analysis a ThermoFisher Scientific K-ALPHA spectrometer, which was equipped with a monochromated Al-K α source ($h\nu = 1486.6$ eV) and a 200 μ m X-ray spot size, was used. To gather comprehensive spectra, the particulate samples were pressed onto indium foils, then the instrument collected data with a constant pass energy of 200 eV spanning the range of 0-800 eV. High-resolution spectra were obtained using a constant pass energy of 40 eV. Charge neutralization was utilized throughout the analysis process, and depth profiles were produced using an Ar⁺ ion gun with 360s of sputtering incorporated between each profiling level. High-resolution spectra for core levels including Si_{2p}, C_{1s} and O_{1s} were obtained using ThermoFisher Scientific's Avantage software and applying Scofield sensitivity factors. To maintain the preservation of binding energies, initial XPS spectra were captured prior to the start of the sputtering process. Minimal Ar⁺ sputtering was performed to remove any surface impurities and ensure that there is a consistent elemental composition at all depths of the material.

2.3.4. TEM analysis

Samples of coated and heat-treated particles were embedded in epoxy resin, cut with a wire saw, and mechanically thinned to a thickness of approximately 100 μ m. These thin cross sections containing coated and heat-treated fibers were then processed using Ar⁺ ion beam milling (JEOL, IonSlicer, EM-09100IS) until electron transparency was achieved. The study employed conventional Transmission Electron Microscopy (TEM) to analyze samples using Bright-Field (BF) and Dark-Field (DF) modes. The CM30ST microscope (Philips, Thermofischer) was used, operating at 300 kV with a LaB₆ source. The DF images were generated via electron beam scattering from *sp*²-C basal atomic layers spaced between 0.3 and 0.4 nm and SiC basal atomic layers spaced between 0.2 and 0.3 nm. Selected Area Diffraction (SAD) patterns were acquired from areas of 400 nm diameter to determine the microstructural organization.

3. Results and discussion

Scanning Electron Microscopy images (see Figure 1) of the BN/SiC_x coatings show remarkable uniformity in thickness throughout the entire surface of the particles (see Figure 1.a). It is crucial to highlight the BN deposit's lack of alterations, breaks, or damage. The uninterrupted continuity indicates the deposition process's robustness and the stability of operating conditions during different coating stages. Consistency in this regard is vital to ensure the integrity of superimposed layers, especially in the case of multilayer coatings or laminated composite structures. The lack of degradation between

consecutive layers ensures that composite material properties remain constant, preventing the formation of weak spots and ensuring dependable performance throughout the coating's thickness. This coherence is indicative of the high quality of the coating obtained through the FB-CVD deposition process. SEM images of the intentionally flaked coating (see Figure 1.b) display the undamaged BN lower layer and SiC_x upper layer on the particles. Finally, the cold copper pelletized and polished preparation (see Figure 1.c) assesses the homogeneity of the material, the SiC_x coating is approximately 500 nm thick on all particles observed and the BN interphase remains adherent to the particles under the pre-matrix coating.

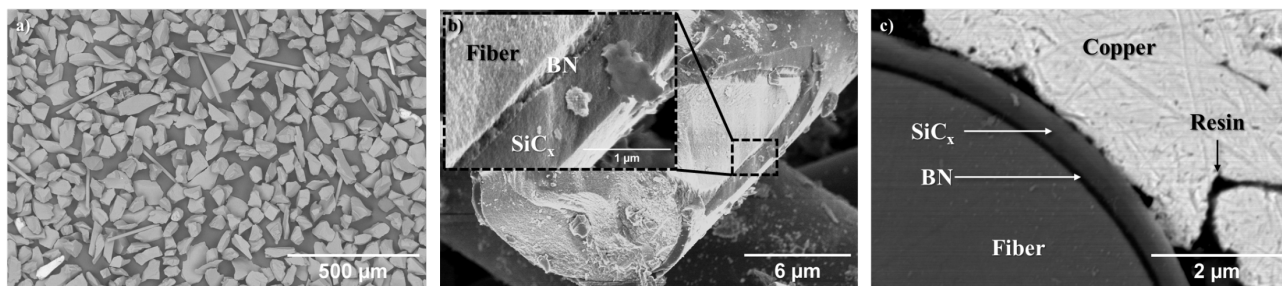


Figure 1 : a) SEM-BSE image of the coating at the reactor discharge (undamaged), b) SEM-SE images of the BN/SiC_x coatings deliberately flaked (to reveal the coatings) and c) SEM-BSE image of the BN/SiC_x coating cold-pelletized in copper (cut and polished).

Energy Dispersive Spectroscopy analyses confirm the preservation of the BN and SiC_x layers and provide data on the approximate atomic content of the last coating (see Figure 2). These results demonstrate a consistent match with the expected compositions of the coatings, which is necessary to assess the conformity of successive deposits and maintain the consistency of the chemical properties of the coated materials. EDX analysis conducted on the coated particles at the reactor outlet indicates that the concentration comprises of about 20%_{at.} silicon and 80%_{at.} carbon.

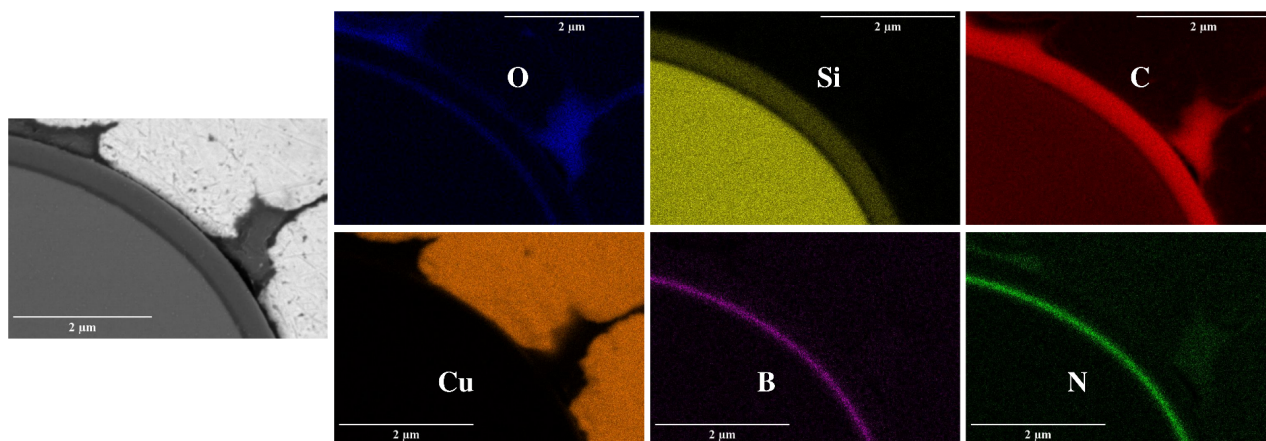


Figure 2 : EDX mapping of the polished cross-section of the BN/SiC_x coated fiber crimped in copper.

The atomic concentrations of silicon and carbon, as determined by Auger spectroscopy, exhibit the same stoichiometry compared to those obtained through EDX with SiC_x coating with $x = 4$. Nevertheless, the examination of the profile line (see Figure 3) consistently verifies the integrity of the BN deposit underlying the SiC_x deposit. The atomic environment of the SiC_x coating is subjected to XPS analysis following the etching of the surface of the particles (see Figure 4). Figure 4 show deconvolutions of the XPS spectra within the silicon, carbon, and oxygen regions. In the silicon spectrum (Si_{2p}, see Figure 4.a), predominant Si-C₄ bonds are observed, constituting up to 19%_{at.} atomic concentration, with less frequent silicon bonds involving carbon and oxygen, accounting for up to 1%_{at.} atomic concentration. The deconvolution of the carbon spectrum (C_{1s}, see Figure 4.b) reveals a complex structure, indicative of a diverse array of carbon bonds. Peaks are centered around C-Si₄, C-C, C-CO, and C-O environments. Notably, the deconvolution identifies a primary peak at 284.5 eV, assigned to the C-C *sp*² environment, representing over 46%_{at.}. The second most prevalent bond is attributed to C-Si₄ bonds, comprising 22%_{at.}. The remaining carbon forms bonds with oxygen, reaching up to 9%_{at.}. Finally, the oxygen atomic environment (O_{1s}, see Figure 4.c) suggests bonds with silicon and carbon of less than 2%_{at.}

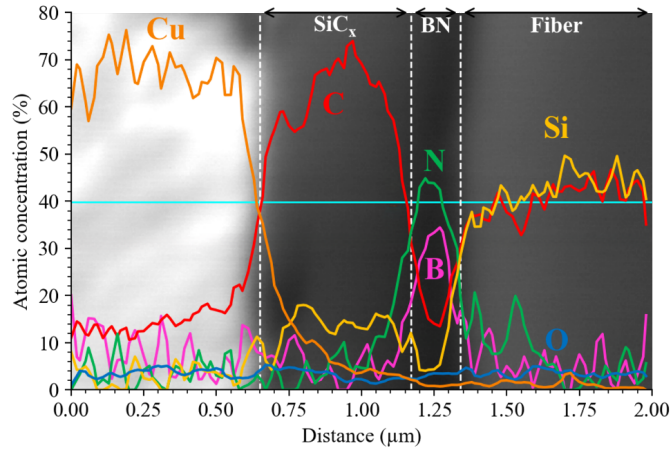


Figure 3 : Auger profil spectroscopy of the BN/SiC_x coated fiber crimped in copper (SEM-BSE image).

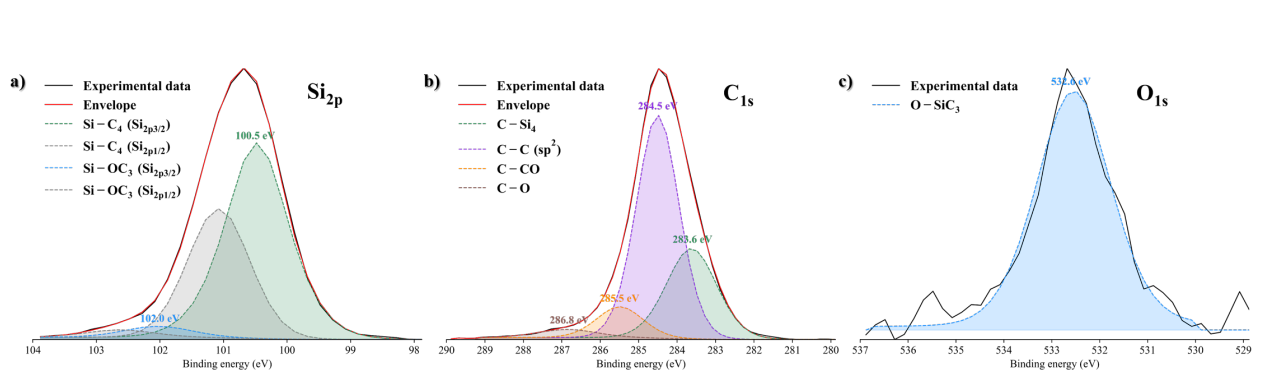


Figure 4 : XPS deconvolution of the Si, C and O spectra obtained within the SiC_x coating.

Table 1 : Summary of elements and chemical bonds detected by XPS with fit characteristics and atomic proportions.

Element/Bonding	Peak (eV)	FWHM (eV)	Area (CPS.eV)	Concentration (% _{at})
Si_{2p}				20.57
Si-C ₄ (Si _{2p3/2})	100.47	1.17	12901.69	19.45
Si-C ₄ (Si _{2p1/2})	101.07	1.15	7995.52	0.00
Si-OC ₃ (Si _{2p3/2})	102.02	1.26	744.39	1.12
Si-OC ₃ (Si _{2p1/2})	102.62	1.26	491.89	0.00
C_{1s}				77.59
C-C (<i>sp</i> ²)	284.50	1.31	50788.02	46.24
C-Si ₄	283.63	1.54	24276.05	22.09
C-CO	285.49	1.42	7632.90	6.95
C-OH	286.85	1.82	2527.93	2.31
O_{1s}				1.84
O-SiC ₃	532.55	1.83	4969.72	1.84

150

The SiC_x deposit is subjected to analysis through transmission electron microscopy (see Figure 5). Following FB-CVD elaboration, BF images of the deposits suggest a slightly stratified structure, with areas exhibiting uniformly distributed variations in brightness (see Figure 5.a). To simulate high-temperature behavior, BN/SiC_x undergo thermal treatment at 1450 °C for 2 hours under 1 bar of argon. TEM and EDX observations demonstrate that the morphological state and surface elemental composition suggest that the thermal treatment has preserved the chemical integrity of the deposits with a SiC_x coating with $x = 4$ again. However, the microstructure has evolved significantly. BF images (see Figure 5.b) reveal that the SiC_x deposit consists of parallel layers to the fiber surface, alternating between dark and light layers. DF images of *sp*² carbon at 002 (see Figure 5.c) and silicon carbide at 111 (see Figure 5.d) confirm the presence of layers corresponding to regions rich in silicon carbide or carbon. Electron diffractions exhibit characteristic SiC

155

160 rings at 2.42 Å and 2.52 Å (characteristic of the 111 direction of nanocrystalline SiC-β) and a more diffuse ring at 3.52 Å characteristic of sp^2 carbon layers. Figure 5.e illustrates the simultaneous presence of DF-illuminated regions associated with sp^2 carbon (depicted in black) and SiC (depicted in yellow) within a single image. The stratified structure is clearly discernible, characterized by alternating layers containing turbostratic sp^2 carbon and crystallized SiC grains. Regarding the BN ex-TEAB deposit, there are no significant changes in its structure or texture.

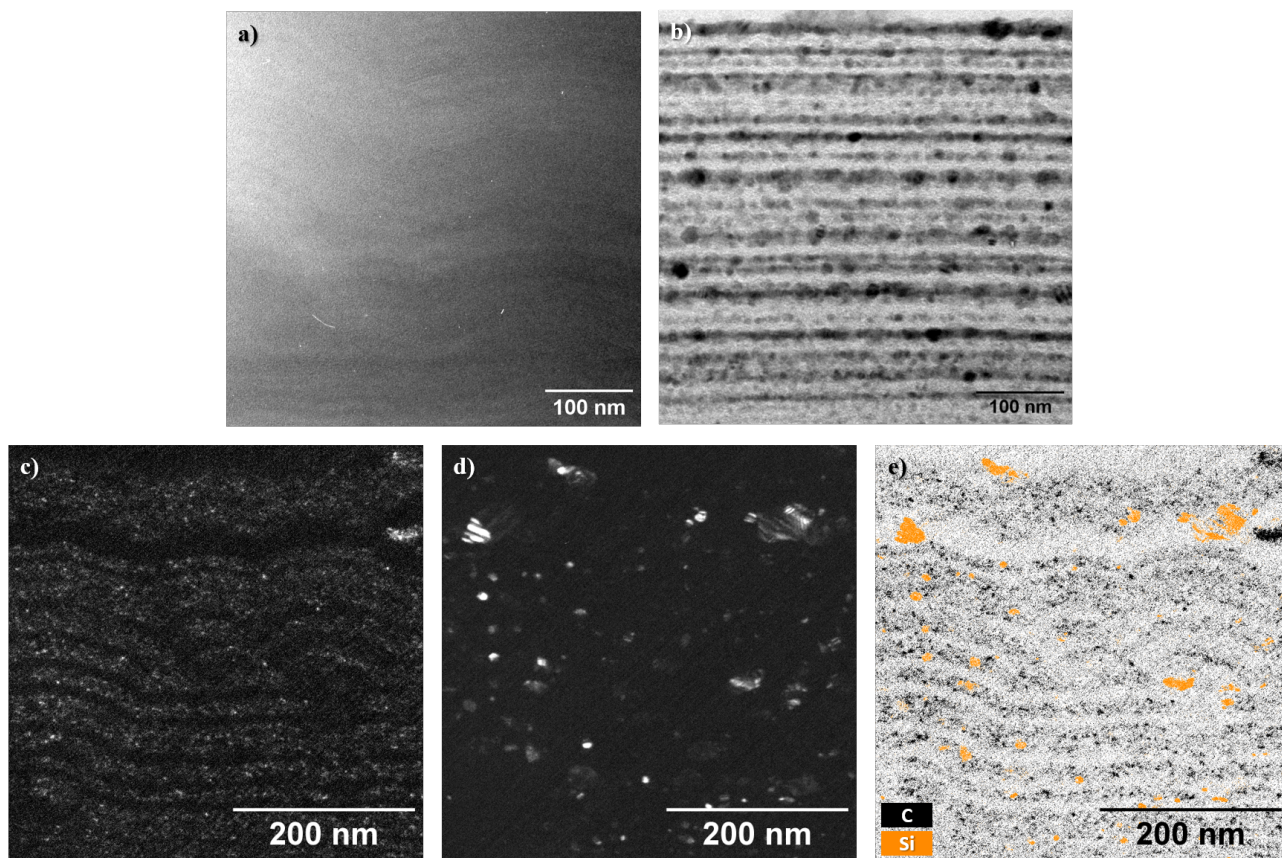


Figure 5 : TEM-BF analysis of a SiC_x coating: a) after elaboration and b) after high-temperature treatment. TEM-DF c) 002 (PyC) and d) 111 (SiC). e) Combined MET-DF 002 (in black) and 111 (in yellow) images.

165 This distinctive structure can be explained by the specific geometry of the fluidized bed reactor. In the CVD process, the reactive gas mixture, blended with the carrier gas, is introduced at the bottom of the column, passes through the porous distributor ensuring uniform gas distribution, and then comes into contact with the solid phase throughout the height of the bed driven by the gas flow. The hot zone extends over the entire height of the bed, providing the necessary energy for both the precursor's decomposition and its maturation. The maturation is more advanced when the precursor species remains in this reactive hot zone for an extended period. In practice, when the precursor is sufficiently decomposed to allow for deposition on the particles, and the gas phase is in sufficiently intimate contact with the solid phase, a portion of the gas phase initially forms a siliceous deposit (silicon coating being thermodynamically more favorable [32]). The other part of this gas phase continues to mature under the influence of temperature, undergoing a series of more advanced chemical reactions. Among these, ethyl groups decompose and form a more carbonaceous deposit [33]. These reactions occur at different maturation stages, resulting in deposits forming at different heights in the fluidized bed. This hypothesis has been validated through *in-situ* deposits on fixed substrates placed at various heights in the fluidized bed. Stoichiometric silicon carbide deposits were found in the first centimeters of the bed, gradually becoming contaminated with excess carbon at higher elevations. During fluidization, particles successively encounter the upper and lower regions of the bed due to their agitation. Consequently, particles encounter environments conducive to both carbonaceous and siliceous deposits, giving rise to the appearance of this stratified structure alternating between carbon-rich and silicon-rich zones.

4. Conclusion

180 In conclusion, this study explores the utilization of triethylsilane as a non-halogenated and less hazardous precursor for the Fluidized Bed – Chemical Vapor Deposition process in depositing silicon carbide on short fibers. The focus is on characterizing the pre-matrix SiC coating on a boron nitride interphase, aiming to enhance the understanding of these coatings for their potential application in short-fiber-reinforced SiC/SiC CMCs. The experimental procedures involved FB-CVD coating using TES as a single-source SiC precursor, high-temperature treatments, and comprehensive characterizations through various techniques, including SEM/EDX, Auger, XPS and TEM analysis.

SEM images demonstrate the uniformity and robustness of the SiC_x coating, with particular attention to the preservation of the underlying BN layer. EDX analyses confirm the expected compositions of the coatings, crucial for assessing the conformity of successive deposits. Auger spectroscopy provides insights into the atomic concentration of SiC_x, and XPS analysis delves into the atomic environment of the SiC_x coating mainly composed of C-C and C-Si₄ bonds. TEM analysis offer a detailed examination of coated and heat-treated particles, revealing a distinctive stratified structure with alternating carbon-rich and silicon-rich zones.

The study highlights the potential of TES as a precursor for SiC deposition, addressing concerns related to halogenated precursors' disadvantages. The results contribute valuable insights into the FB-CVD process for short-fiber coating, offering a pathway for tailoring coatings. Further research could explore optimization strategies for achieving precise control over coating properties and enhancing the performance of these coatings in demanding applications within the aerospace industry and beyond.

Acknowledgements

The authors wish to express their gratitude for the significant contributions of Sébastien Couthures and Rémi Bouvier in the maintenance of the fluidized bed reactor. The authors also thank the University of Bordeaux for granting financial support and Safran Ceramics for their operational assistance. Furthermore, the authors would like to acknowledge the contribution of Christine Labrugère and Mélanie Vaudescal from PLACAMAT for the X-Ray Photoelectron Spectroscopy and Auger Electron Spectroscopy analysis.

Declaration of interests

The authors declare that they have no known competing financial interests or personal relationships that could have appeared to influence the work reported in this paper.

References

- [1] F. Christin, Design, Fabrication, and Application of Thermostructural Composites (TSC) like C/C, C/SiC, and SiC/SiC Composites, *Adv. Eng. Mater.* 4 (2002) 903–912. <https://doi.org/10.1002/adem.200290001>.
- [2] R.R. Naslain, SiC-Matrix Composites: Nonbrittle Ceramics for Thermo-Structural Application, *Int. J. Appl. Ceram. Technol.* 2 (2005) 75–84. <https://doi.org/10.1111/j.1744-7402.2005.02009.x>.
- [3] J.C. Cavalier, I. Berdoyes, E. Bouillon, Composites in Aerospace Industry, *Adv. Sci. Technol.* 50 (2006) 153–162. <https://doi.org/10.4028/www.scientific.net/AST.50.153>.
- [4] R. Weiss, M. Henrich, Short-Fiber Reinforced CMCS: Potentials and Problems, in: *Mech. Prop. Perform. Eng. Ceram. Compos. Ceram. Eng. Sci. Proc.*, John Wiley & Sons, Ltd, 2005: pp. 351–359. <https://doi.org/10.1002/9780470291221.ch42>.
- [5] Y. Shi, J.-M. Hausherr, H. Hoffmann, D. Koch, Inspection of geometry influence and fiber orientation to characteristic value for short fiber reinforced ceramic matrix composite under bending load, *J. Eur. Ceram. Soc.* 37 (2017) 1291–1303. <https://doi.org/10.1016/j.jeurceramsoc.2016.11.042>.
- [6] R.R. Naslain, The design of the fibre-matrix interfacial zone in ceramic matrix composites, *Compos. Part Appl. Sci. Manuf.* 29 (1998) 1145–1155. [https://doi.org/10.1016/S1359-835X\(97\)00128-0](https://doi.org/10.1016/S1359-835X(97)00128-0).
- [7] S. Jacques, A. Lopez-Marure, C. Vincent, H. Vincent, J. Bouix, SiC/SiC minicomposites with structure-graded BN interphases, *J. Eur. Ceram. Soc.* 20 (2000) 1929–1938. [https://doi.org/10.1016/S0955-2219\(00\)00064-9](https://doi.org/10.1016/S0955-2219(00)00064-9).
- [8] F. Rebillat, A. Guette, C.R. Brosse, Chemical and mechanical alterations of SiC Nicalon fiber properties during the CVD/CVI process for boron nitride, *Acta Mater.* 47 (1999) 1685–1696. [https://doi.org/10.1016/S1359-6454\(99\)00032-4](https://doi.org/10.1016/S1359-6454(99)00032-4).
- [9] S. Jacques, H. Vincent, C. Vincent, A. Lopez-Marure, J. Bouix, Multilayered BN Coatings Processed by a Continuous LPCVD Treatment onto Hi-Nicalon Fibers, *J. Solid State Chem.* 162 (2001) 358–363. <https://doi.org/10.1006/jssc.2001.9387>.
- [10] Y. Cheng, X. Yin, Y. Liu, S. Li, L. Cheng, L. Zhang, BN coatings prepared by low pressure chemical vapor deposition using boron trichloride–ammonia–hydrogen–argon mixture gases, *Surf. Coat. Technol.* 204 (2010) 2797–2802. <https://doi.org/10.1016/j.surfcoat.2010.02.046>.
- [11] P. Carminati, T. Buffeteau, N. Daugey, G. Chollon, F. Rebillat, S. Jacques, Low pressure chemical vapour deposition of BN: Relationship between gas phase chemistry and coating microstructure, *Thin Solid Films* 664 (2018) 106–114. <https://doi.org/10.1016/j.tsf.2018.08.020>.
- [12] A. Figueras, S. Garelik, J. Santiso, R. Rodriguez-Clemente, B. Armas, C. Combescure, R. Berjoan, J.M. Saurel, R. Caplain, Growth and properties of CVD-SiC layers using tetramethylsilane, *Mater. Sci. Eng. B* 11 (1992) 83–87. [https://doi.org/10.1016/0921-5107\(92\)90196-G](https://doi.org/10.1016/0921-5107(92)90196-G).
- [13] A.D. Johnson, J. Perrin, J.A. Mucha, D.E. Ibbotson, Kinetics of silicon carbide CVD: surface decomposition of silacyclobutane and methylsilane, *J. Phys. Chem.* 97 (1993) 12937–12948. <https://doi.org/10.1021/j100151a049>.
- [14] W.G. Zhang, K.J. Hüttinger, CVD of SiC from Methyltrichlorosilane. Part I: Deposition Rates, (n.d.) 6.

- 230 [15] T. Da Calva Mouillevois, C. Rivière, G. Chollon, G. Vignoles, N. Bertrand, Gaseous fluidization of short fibers and powders, influence of temperature and pressure, *Chem. Eng. J.* 453 (2023) 139612. <https://doi.org/10.1016/j.cej.2022.139612>.
- [16] T. Da Calva Mouillevois, M. Audren-Paul, G. Chollon, N. Bertrand, Fluidization of variable short fiber/powder mixtures: Hydrodynamic investigation, *Chem. Eng. J.* (2023) 144846. <https://doi.org/10.1016/j.cej.2023.144846>.
- 235 [17] S. Kouadri-Mostefa, P. Serp, M. Hémati, B. Caussat, Silicon Chemical Vapor Deposition (CVD) on microporous powders in a fluidized bed, *Powder Technol.* 120 (2001) 82–87. [https://doi.org/10.1016/S0032-5910\(01\)00351-5](https://doi.org/10.1016/S0032-5910(01)00351-5).
- [18] L. Cadoret, N. Reuge, S. Pannala, M. Syamlal, C. Coufort, B. Caussat, Silicon CVD on powders in fluidized bed: Experimental and multifluid Eulerian modelling study, *Surf. Coat. Technol.* 201 (2007) 8919–8923. <https://doi.org/10.1016/j.surfcoat.2007.04.119>.
- [19] F. Vanni, B. Caussat, C. Ablitzer, X. Iltis, M. Bothier, Silicon coating on very dense tungsten particles by fluidized bed CVD for nuclear application, *Phys. Status Solidi A* 212 (2015) 1599–1606. <https://doi.org/10.1002/pssa.201532304>.
- 240 [20] S. Le Gallet, G. Chollon, F. Rebillat, A. Guette, X. Bourrat, R. Naslain, M. Couzi, J.L. Bruneel, Microstructural and microtextural investigations of boron nitride deposited from BCl₃-NH₃-H₂ gas mixtures, *J. Eur. Ceram. Soc.* 24 (2004) 33–44. [https://doi.org/10.1016/S0955-2219\(03\)00126-2](https://doi.org/10.1016/S0955-2219(03)00126-2).
- [21] S. Prouhet, A. Guette, F. Langlais, An Experimental Kinetic Study Of Boron Nitride CVD From BF₃-NH₃-Ar Mixtures, *J. Phys. IV* 02 (1991) C2-119-C2-126. <https://doi.org/10.1051/jp4:1991214>.
- 245 [22] H. Pedersen, S. Leone, A. Henry, F.C. Beyer, V. Darakchieva, E. Janzén, Very high growth rate of 4H-SiC epilayers using the chlorinated precursor methyltrichlorosilane (MTS), *J. Cryst. Growth* 307 (2007) 334–340. <https://doi.org/10.1016/j.jcrysgro.2007.07.002>.
- [23] O. Kordina, C. Hallin, A. Ellison, A.S. Bakin, I.G. Ivanov, A. Henry, R. Yakimova, M. Touminen, A. Vehanen, E. Janzén, High temperature chemical vapor deposition of SiC, *Appl. Phys. Lett.* 69 (1996) 1456–1458. <https://doi.org/10.1063/1.117613>.
- 250 [24] A. Mallikarjunan, A.D. Johnson, M. Wang, R.N. Vrtis, B. Han, X. Lei, M.L. O’neill, Methods for Making Silicon Containing Films on Thin Film Transistor Devices, EP2823083 (B1), 2023. <https://worldwide.espacenet.com/publicationDetails/biblio?FT=D&date=20231004&DB=EPODOC&locale=&CC=EP&NR=2823083B1&KC=B1&ND=1> (accessed November 10, 2023).
- [25] J. Niemann, W. Bauhofer, Properties of a-Si_{1-x}C_xH thin films deposited from the organosilane Triethylsilane, *Thin Solid Films* 352 (1999) 249–258. [https://doi.org/10.1016/S0040-6090\(99\)00320-X](https://doi.org/10.1016/S0040-6090(99)00320-X).
- 255 [26] H. Okada, M. Kato, T. Ishimaru, M. Furukawa, H. Sekiguchi, A. Wakahara, Organometallic chemical vapor deposition of silicon nitride films enhanced by atomic nitrogen generated from surface-wave plasma, *AIP Conf. Proc.* 1585 (2014) 64–67. <https://doi.org/10.1063/1.4866620>.
- [27] S. Guruvenket, S. Andrie, M. Simon, K.W. Johnson, R.A. Sailer, Atmospheric Pressure Plasma CVD of Amorphous Hydrogenated Silicon Carbonitride (a-SiCN:H) Films Using Triethylsilane and Nitrogen, *Plasma Process. Polym.* 8 (2011) 1126–1136. <https://doi.org/10.1002/ppap.201100035>.
- 260 [28] S. Guruvenket, S. Andrie, M. Simon, K.W. Johnson, R.A. Sailer, Atmospheric-Pressure Plasma-Enhanced Chemical Vapor Deposition of a-SiCN:H Films: Role of Precursors on the Film Growth and Properties, *ACS Appl. Mater. Interfaces* 4 (2012) 5293–5299. <https://doi.org/10.1021/am301157p>.
- [29] H. Sakaue, M. Nakano, T.I.T. Ichihara, Y.H.Y. Horiike, Digital Chemical Vapor Deposition of SiO₂ Using a Repetitive Reaction of Triethylsilane/Hydrogen and Oxidation, *Jpn. J. Appl. Phys.* 30 (1991) L124. <https://doi.org/10.1143/JJAP.30.L124>.
- 265 [30] A. El Mansouri, N. Bertrand, S. Couthures, A. Guette, Apparatus for Fluidized-Bed Chemical Vapour Deposition, WO2022003268 (A1), 2022. https://worldwide.espacenet.com/publicationDetails/biblio?FT=D&date=20220106&DB=EPODOC&locale=fr_EP&CC=WO&NR=2022003268A1&KC=A1&ND=4 (accessed April 2, 2022).
- 270 [31] T. Da Calva Mouillevois, C. Rivière, H. Plaisantin, J. Roger, T. Hungria, G. Chollon, N. Bertrand, Towards Controlled Fluidized Bed – Chemical Vapor Deposition of Boron Nitride: Thermochemical Analysis and Microstructural Investigations, *Adv. Mater. Interfaces* (n.d.). <https://doi.org/10.1002/admi.202400452>.
- [32] D.-H. Nam, B.G. Kim, J.-Y. Yoon, M.-H. Lee, W.-S. Seo, S.-M. Jeong, C.-W. Yang, W.-J. Lee, High-Temperature Chemical Vapor Deposition for SiC Single Crystal Bulk Growth Using Tetramethylsilane as a Precursor, *Cryst. Growth Des.* 14 (2014) 5569–5574. <https://doi.org/10.1021/cg5008186>.
- 275 [33] S.J. Cassady, R. Choudhary, N.H. Pinkowski, J. Shao, D.F. Davidson, R.K. Hanson, The thermal decomposition of ethane, *Fuel* 268 (2020) 117409. <https://doi.org/10.1016/j.fuel.2020.117409>.

Vitae



Thomas Da Calva Mouillevois is a Ph.D. graduate from the University of Bordeaux. He is working on the development of ceramic coatings and short fibers fluidization at the ThermoStructural Composites Laboratory since 2020. Graduated from the National Engineering School of Tarbes, France in the speciality of Structural Materials and Processes Engineering, Thomas Da Calva also holds a double degree in Materials Processing Characterization and Surface Treatments in partnership with the National School of Chemical and Technological Arts Engineers and the Paul Sabatier University of Toulouse.